Interplay between Gelation and Phase Separation in Aqueous Solutions of Methylcellulose and Hydroxypropylmethylcellulose

ARTICLE *in* LANGMUIR · JUNE 2012

Impact Factor: 4.46 · DOI: 10.1021/la300971r · Source: PubMed

6 AUTHORS, INCLUDING:

Patrick Fairclough
The University of Sheffield
100 PUBLICATIONS **2,967** CITATIONS
SEE PROFILE

Hao Yu
The University of Sheffield
3 PUBLICATIONS **18** CITATIONS
SEE PROFILE

Anthony Ryan
The University of Sheffield
317 PUBLICATIONS **11,066** CITATIONS
SEE PROFILE

Michael J. Radler
Dow Chemical Company
22 PUBLICATIONS **121** CITATIONS
SEE PROFILE

Langmuir

Article

pubs.acs.org/Langmuir

Interplay between Gelation and Phase Separation in Aqueous Solutions of Methylcellulose and Hydroxypropylmethylcellulose

J. Patrick A. Fairclough,*[,†] Hao Yu,*[,†] Oscar Kelly,[†,⊥] Anthony J. Ryan,[†] Robert L. Sammler,[‡] and Michael Radler[§]

[†]Department of Chemistry, The University of Sheffield, Sheffield S3 7HF, U.K.

[‡]Material Science and Engineering Laboratory, The Dow Chemical Company, Midland, Michigan 48674, United States

[§]Dow Construction Chemicals, The Dow Chemical Company, Midland, Michigan 48674, United States

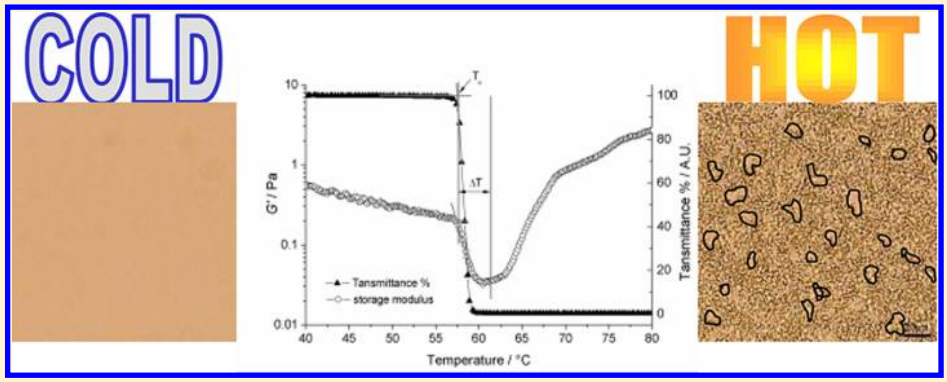

ABSTRACT: Thermally induced gelation in aqueous solutions of methylcellulose (MC) and hydroxypropylmethylcellulose (HPMC) has been studied by rheological, optical microscopy, and turbidimetry measurements. The structural and mechanical properties of these hydrogels are dominated by the interplay between phase separation and gelation. In MC solutions, phase separation takes place almost simultaneously with gelation. An increase in the storage modulus is coupled to the appearance of a bicontinuous structure upon heating. However, a thermal gap exists between phase separation and gelation in the case of HPMC solutions. The storage modulus shows a dramatic decrease during phase separation and then rises in the subsequent gelation. A macroporous structure forms in the gels via "viscoelastic phase separation" linked to "double phase separation".

1. INTRODUCTION

Methylcellulose (MC) and hydroxypropylmethylcellulose (HPMC) are important commercial cellulose ethers that have been widely used in personal care products,[1,2] foods,[3−5] pharmaceutical applications,[6−12] and construction materials.[13,14] Unusually, aqueous solutions of these materials exhibit inverse solubility−temperature behavior, where the polymer solubility decreases with increasing temperature above a lower critical solution temperature (LCST). The solutions undergo a sol−gel transition upon heating, returning to a solution state on cooling. Furthermore, the gelation of such a system is coupled to an increase in turbidity due to phase separation. To date, the gelation mechanism of MC and HPMC is still poorly understood, although many hypotheses have been proposed. Gel formation has been generally accepted as a competition between hydrophilic and hydrophobic interactions.[15−18] The hypothesis is that at a low-temperature water molecules form a "cage structure"[19−21] around hydrophobic segments along the polymer chains to raise the solubility of polymer in water. With increasing temperature hydrogen bonds become weaker and the "cage structure" is sufficiently disrupted at the gelation temperature to facilitate phase separation. The exposed but still hydrated hydrophobic segments subsequently aggregate together, forming a bicontinuous network.

The structural and rheological properties of MC and HPMC gels have been extensively studied since 1935.[22−24]Recently, Takeshita et al.[25] investigated the evolution of structure with time in aqueous solutions of MC by small-angle light scattering (SALS). The data indicate that liquid−liquid phase separation takes place via spinodal decomposition. Furthermore, Villetii et al.[26] found that in MC/NaCl solutions the mechanism of phase separation is also spinodal decomposition. Kita et al. reported[27,28] that phase separation is limited by gelation in HPMC solutions. They suggest that a spontaneous pinning of spinodal decomposition occurs, as the structure formed in a shallower quench has a larger domain length than that formed by a deeper quench. On the other hand, it was found that MC hydrogels provide a much higher gel modulus than HPMC hydrogels; the former are normally considered as "firm gels" and the latter as "weak gels". Interestingly, the development of moduli in aqueous MC is dramatically different than that in

Received: March 6, 2012
Revised: June 11, 2012
Published: June 13, 2012

aqueous HPMC during the sol−gel transition.[29−32] For HPMC solutions, as temperature is raised, a sudden drop in the storage modulus is observed followed by an increase as gelation occurs. In contrast, for MC solutions no sharp drop appears, and the solutions merely thicken as temperature is increased.

Structural information in physical gels has attracted a great deal of interest because it is associated with the physicochemical formation of network junction points as well as the fundamental properties of gels. According to Flory's structural classification,[33] thermoreversible gels generally belong to the third type, in which "networks formed through physical aggregation, predominantly disordered, but with regions of local order". Te Nijenhuis[34] subdivided thermoreversible gels into different groups based on the mechanisms of physical interactions. For some synthetic polymers such as poly(vinyl chloride) and poly(vinyl alcohol), crystallization forms network junctions during gelation.[35] In many biopolymer gels, including gelatin, agarose, and carrageenans, the helix−coil transition causes the formation of a continuous network.[36,37] Phase separation is observed in atactic polystyrene and some block copolymer solutions during gel formation.[38] In other cases, gelation can be induced by complex formation[39] or mesogenic interactions.[40] We found that for both MC and HPMC materials phase separation occurs prior to gelation. Hence, it is proposed that phase separation is responsible for gelation in these systems.

Although the thermal gelation behavior of aqueous cellulose ethers has been intensively studied in the past,[41,42] there has been little work on the interplay between phase separation and gelation. The aim of this article is to explore the growth of gel modulus and the development of structure upon heating, with the goal of understanding the complex thermal behavior of these systems. The rheological behavior of MC and HPMC solutions during gelation was monitored by using rheology, whereas the development of structure was probed independently by optical microscopy. As these experiments were performed under a similar thermal program, it is possible to reveal the relationship between structural and mechanical properties during the coupling process of gelation and phase separation.

2. EXPERIMENTAL SECTION

2.1. Materials. Figure 1 shows chemical structures of methylcellulose (MC) and hydroxypropylmethylcellulose (HPMC) consisting of anhydroglucose units with various substituents. For both materials, the degree of substitution (DS) identifies the average number of methoxyl groups per anhydroglucose unit. Additionally, the molar substitution (MS) describes the number of moles of hydroxypropyl groups per mole of anhydroglucose unit for HPMC. Table 1 lists METHOCEL (trademark of The Dow Chemical Company) cellulosic ether materials that were provided by The Dow Chemical Company. In order to compare the gelation properties of one material with another, the materials were chosen to have similar molecular weights and polydispersities. Polydimethylsiloxane oil was purchased from Aldrich and used as received.

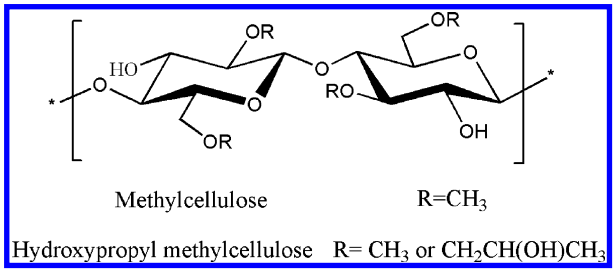

Figure 1. Chemical structure of methylcellulose and hydroxypropylmethylcellulose.

Table 1. Molecular Information of Methylcellulose (MC) and Hydroxypropylmethylcellulose (HPMC) Products

product	type	DS	MS	M_w[a]/g·mol^{-1}	M_w/M_n[b]
MC	A4M FG[c]	1.8		271 500	3.4
HPMC	E4M FG	1.9	0.25	323 200	4.1

[a]The weight-average molecular weight as determined by GPC. [b]The polydispersity index. [c]FG denotes food grade.

2.2. Solution Preparation. The supplied MC and HPMC contain approximately 2−5 wt % of water. In order to prepare solutions at the target concentrations, materials were dried in a vacuum oven at 70 °C overnight to remove the residual water. Solutions of cellulose ethers were prepared by a "hot water" method to prevent powder agglomeration during dissolution. Approximately half the required volume of deionized water was heated to 80 °C; the preweighed material was then introduced to the hot water under vigorous stirring. Once the predried powder was thoroughly dispersed, the remainder of the water was added and the temperature of mixture was lowered to 5 °C via an ice bath. The mixture was continuously stirred at 5 °C until a transparent solution was observed. Subsequently, a small amount of deionized water was added to compensate for water evaporation during solution preparation. Solutions were kept in a refrigerator overnight for full hydration. Air bubbles in the solutions were then minimized under vacuum. All solutions were stored in the refrigerator at 5 °C before use.

2.3. Turbidimetric Measurements. Turbidimetric measurements were carried out at a wavelength of 500 nm using a UV−vis spectrophotometer (Cary 100). The solution was added into a standard 1 × 1 × 5 cm^3 cuvette and then placed in a thermostated multicell holder. Deionized water was used as a reference. Both sample and reference cells were sealed with polydimethylsiloxane oil on the top to minimize water evaporation at high temperatures. The temperature was ramped from 20 to 90 °C and back down to 20 °C at a rate of 1 °C/min. The cloud point was determined by extrapolating the linear region of curve to 100% transmittance.

2.4. Optical Microscopy. Optical microscopy was performed using an Olympus BX50 microscope with a digital CCD camera (Hitachi, KP-D20A). Approximately 2 μL of an aqueous solution was sandwiched between two glass slides, and the periphery was sealed with polydimethylsiloxane oil. Micrographs were recorded by the CCD camera with a ×20 objective. A thermal stage (Linkam THMS600) was used to control the temperature. The solutions were heated from 20 to 90 °C and followed by cooling to 20 °C at a rate of 1 °C/min. In order to avoid glass−solution interface effects, the working distance of the objective was focused on a plane inside the solution, away from the cover glass.

2.5. Rheological Measurements. Rheological measurements were performed on a stress-controlled rheometer (TA AR-G2) with a concentric cylinder (Couette) fixture in an oscillatory mode. Approximately 20 mL of solutions was added to the fixture cell, and 2 mL of polydimethylsiloxane oil was layered over the solution. An additional solvent trap was used to further reduce the rate of water evaporation at high temperatures. For MC solutions, the temperature was ramped from 5 to 90 °C and back down to 5 °C at a rate of 1 °C/min. A frequency of 0.5 Hz and an oscillatory stress of 0.5 Pa were applied. In the case of HPMC solutions, the minimum temperature was increased to 25 °C and the oscillatory stress was reduced to 0.05 Pa.

3. RESULTS AND DISCUSSION

3.1. Gelation. Figure 2a presents the rheology data of a 1.5 wt % A4M solution (MC) during a thermal cycle. The solution

dx.doi.org/10.1021/la300971r | Langmuir 2012, 28, 10551−10557

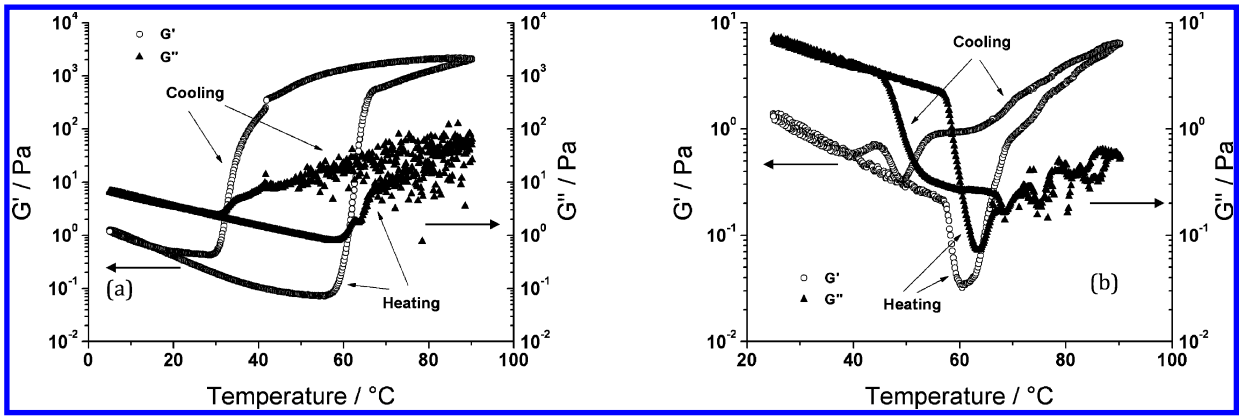

Figure 2. G' and G'' as a function of temperature for aqueous MC (1.5 wt % A4M) (a) and aqueous HPMC (2 wt % E4M) (b) materials. The temperature was cycled from 5 to 90 °C and back down to 5 °C at a rate of 1 °C/min. Measurements were performed using a concentric cylinder fixture (Couette) in an oscillatory mode with a frequency of 0.5 Hz. A constant (oscillatory) stress amplitude of 0.5 Pa was used in a A4M solution and 0.05 Pa in a E4M solution. The horizontal arrows indicate the corresponding axes for the data points.

was heated from 5 to 90 °C and then cooled to 5 °C at a rate of 1 °C/min. Upon heating, the storage modulus, G', was less than the loss modulus, G'', in the range from 5 to 56 °C as the sample was in a liquid solution state. Both moduli decreased with temperature showing "viscosity−temperature correlation".[43,44] After reaching a minimum, a sharp increase, in both G' and G'', was displayed in the data as the polymer chains linked together to create a continuous network. At ∼62 °C, G' became equal to G'', and this crossover point was defined as the gelation temperature, T_{gel}. The development of G' slowed beyond 70 °C until a final value of 2042 Pa was achieved at the maximum temperature of 90 °C. In this region, the logarithm of G' became proportional to temperature. Upon cooling, both G' and G'' fell with decreasing temperature as the preformed continuous network began to dissolve in water. The rate of decrease in the curves increased below 43 °C. When the crossover point of G' and G'' appeared once again, the system transformed from a gel state to a liquid state. This temperature of 33 °C was determined as the dissolution temperature, T_{dis}, in the same manner as T_{gel}. Below 15 °C, the data returned to the original values, indicating that the gel was thermoreversible and water loss during the measurement was insignificant. An obvious thermal hysteresis was observed between the heating and cooling processes due to kinetic effects.

Figure 2b shows the mechanical spectrum of a 2 wt % E4M solution (HPMC). Compared to the A4M solution, there are significant differences in the curves during the sol−gel transition. Both G' and G'' fell as temperature was increased from 25 to 57 °C, but then a dramatic drop was observed in both G' and G'' at higher temperatures. The G' curve decreased rapidly in a narrow temperature region and a minimum appeared at ∼61 °C. Subsequently G' and G'' increased up to the maximum temperature measured of 90 °C. Upon cooling from 90 °C, G' decreased with a similar precipitous drop at 48 °C. The final gel modulus of 6 Pa at 90 °C is 2 orders of magnitude lower than that of the A4M solution. In addition, the E4M solution has a smaller thermal hysteresis with a T_{gel} of 64 °C and a T_{dis} of 52 °C.

In both solutions, the data from the gel regime of G'' suffered from instrumental noise, as the response of the gels was close to the limit of sensitivity of the instrument. If a higher stress was chosen, to improve the G'' signal, then the noise on G' data increased near the sol−gel transition, as defects were generated by the higher stress. Therefore, as G' represents the elastic response, characteristic of a gel, it was felt to be more important to obtain high quality, low noise G' data in the gel regime; thus a low stress was applied.

3.2. Phase Separation. Observation of phase separation in MC and HPMC solutions was performed by optical microscopy with a Linkam hot stage accessory. Figure 3

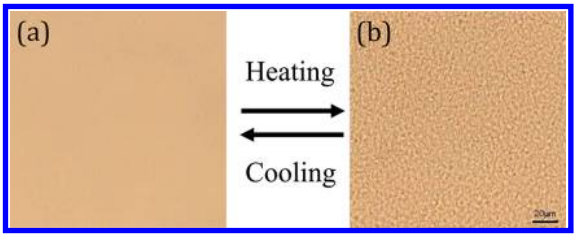

Figure 3. Optical micrographs of the MC solution (1.5 wt % A4M) before and after phase separation: (a) 25 °C, (b) 90 °C. Both images are to the same scale; the scale bar is 20 μm.

presents structures of a MC solution (1.5 wt % A4M) captured before and after phase separation. A homogeneous solution was seen at 25 °C (Figure 3a). While increasing temperature to 90 °C (Figure 3b), phase separation took place through spinodal decomposition to form a bicontinuous structure with polymer-rich and polymer-poor regions. The average distance (the domain length, d) between the two regions was ∼5 μm as determined by a fast Fourier transform (FFT) analysis of the microscope image. Because of the reversible phase behavior, the formed bicontinuous structure was totally dissolved in water when the temperature returned to 25 °C, reproducing the original homogeneous structure.

Unlike MC solutions, the development of structure in HPMC solutions proceeds via a different mechanism. Figure 4 exhibits structures of a 2 wt % E4M solution at 25 (Figure 4a) and 90 °C (Figure 4b). Upon heating, phase separation caused the formation of a complex macroporous structure consisting of a polymer-rich phase, a polymer-poor phase, and an additional water (or possibly an exceedingly polymer-poor) phase. The polymer-rich gel network retains a bicontinuous structure, but the domain length (∼3 μm) was slightly smaller than that in the A4M solution. The additional water phase, in the form of closed macropores randomly dispersed in the sample, has a rough interface between the macropores and the continuous network. Upon cooling this structure disappeared; this

dx.doi.org/10.1021/la300971r | Langmuir 2012, 28, 10551−10557

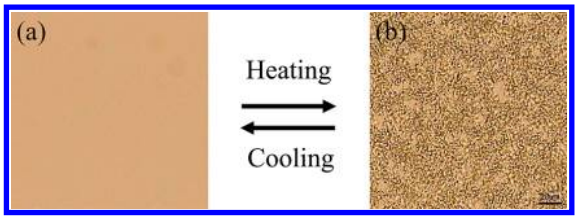

Figure 4. Optical micrographs showing structures of a HPMC solution (2 wt % E4M) before and after phase separation: (a) 25 °C, (b) 90 °C. Both images are to the same scale; the scale bar is 20 μm.

observation was repeated over numerous thermal cycles, just as for the A4M solution.

3.3. Thermodynamic Behavior. Figure 5 displays the coupling process of gelation and phase separation for both MC and HPMC solutions. The growth of G' shows the sol−gel transition upon heating, whereas turbidimetric results reveal the development of structure. A transmittance of 100% was observed in a 1.5 wt % A4M solution at room temperature as the sample was transparent. Phase separation occurred upon heating, the transmittance dropped rapidly over a narrow temperature range from 60 to 65 °C. At even higher temperatures, the transmittance reduced to a minimum as a turbid gel formed. The clouding temperature, T_c, was determined by extrapolating the linear portion of the curve to 100% transmittance, as shown in Figure 5a. It was noticed that this clouding temperature is close to the onset of an increase in G'. In other words, the transparent solution not only becomes turbid with increasing temperature but also transforms to a gel at almost the same time; i.e., phase separation and gelation proceed simultaneously, to within our experimental precision.

Unlike the A4M solution, phase separation and gelation show a distinct separation in a 2 wt % E4M solution (Figure 5b). The clouding temperature correlates well to the significant drop in G', so that phase separation takes place at the same temperature as the modulus reduction. Once a minimum was reached, G' started to grow at higher temperatures. This result shows that gelation proceeds after phase separation for HPMC solutions, and a small thermal gap, ΔT, exists between these two processes.

3.4. Interplay between Gelation and Phase Separation. As outlined above, MC and HPMC solutions exhibit contrasting relationships between gelation and phase separation. Consequently, a combination of mechanical properties and structure is essential to fully understand the interplay of these two processes.

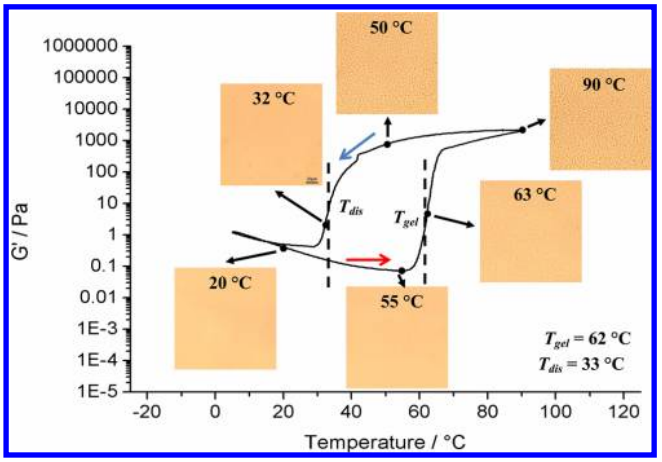

Figure 6. Gel modulus growth and structural formation in a 1.5 wt % A4M solution; the temperature was ramped from 5 to 90 °C and back down to 5 °C at a rate of 1 °C/min. Rheological data were collected independently of the optical microscopy. The red and blue arrow indicate heating and cooling, respectively.

Figure 6 shows development of G' as a function of temperature within a series of optical micrographs for a 1.5 wt % A4M solution. There was no observable structure formed below 55 °C as the temperature of the solution was below T_c. When the solution was warmed to the gelation temperature, 62 °C, a weak bicontinuous structure appeared. A further increase in temperature caused the growth of both gel modulus and phase contrast until the maximum temperature of 90 °C. Upon the subsequent cooling, a decrease in G' was coupled with the weakening of the observed structure. Once the dissolution temperature of 33 °C was reached, the gel returned to a liquid state and the bicontinuous structure disappeared.

It is important to note that the domain length of the bicontinuous structure is independent of temperature in both the heating and cooling processes. This behavior is different to phase separation in nongelling systems, where the domain length increases with time.[45] The result leads us to believe that the gelation in MC solutions prevents further phase separation, a "pinning phenomenon". Hence, the magnitude of the contrast

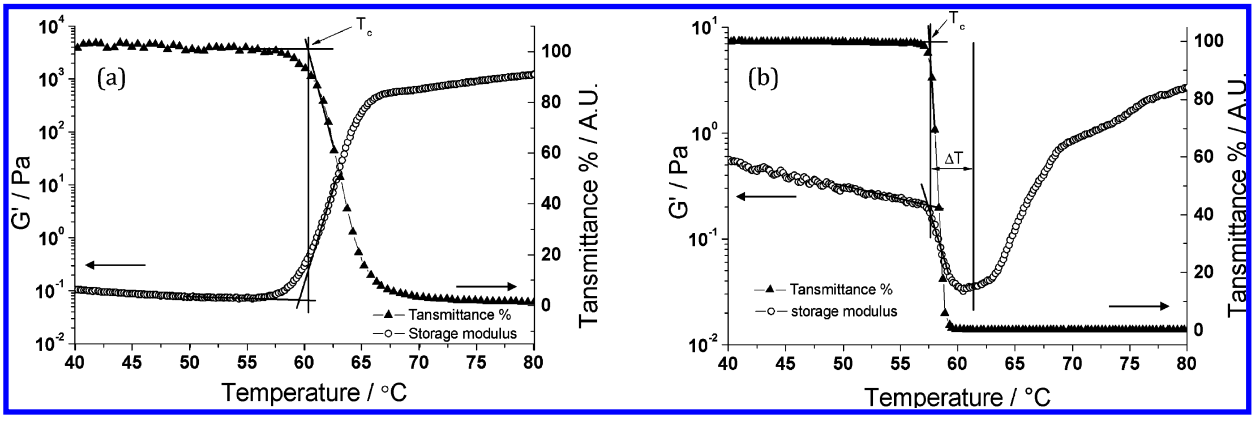

Figure 5. Transmittance and G' as a function of temperature for MC and HPMC solutions; the temperature was ramped from 25 to 90 °C at a rate of 1 °C/min: (a) 1.5 wt % A4M solution; (b) 2 wt % E4M solution. The horizontal arrows indicate the corresponding axes for the data points.

dx.doi.org/10.1021/la300971r | *Langmuir* 2012, 28, 10551−10557

within the images is dependent on temperature, but its size scale is frozen throughout the whole process.

Figure 7 displays thermal behavior of a 2 wt % E4M solution. A weak bicontinuous structure formed at a temperature close to

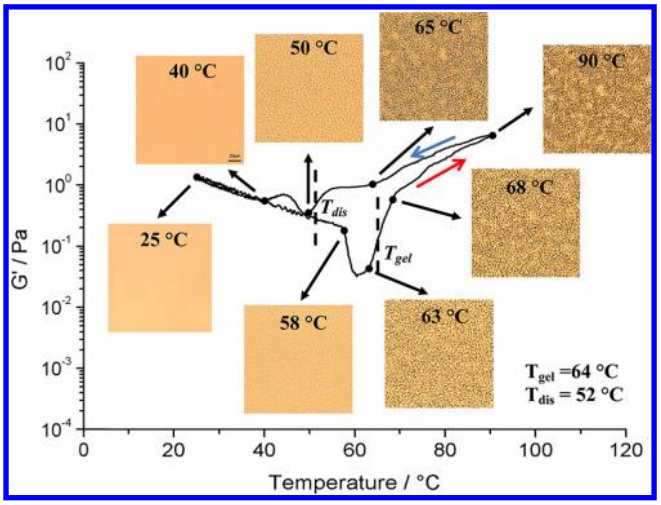

Figure 7. Gel modulus growth and structural formation in a 2 wt % E4M solution; the temperature was ramped from 5 to 90 °C and back down to 5 °C at a rate of 1 °C/min. The red and blue arrows indicate heating and cooling, respectively.

the onset of the drop in G'. This transition temperature was in good agreement with the result obtained by the turbidimetry measurements. Beyond the minimum of G', macropores started to appear over the preformed bicontinuous network accompanying with an increase in G'. In the cooling process, the macropores were "healed" at 50 °C by the swelling of the bicontinuous matrix, and the bicontinuous structure then disappeared at 40 °C. When the G' curve returned to the original position, no structure was observed in the image.

The formation of the complex structure is a result of "viscoelastic phase separation"[46,47] linked to "double phase separation". A liquid−liquid phase separation took place in the solution by spinodal decomposition. The development of structure was then affected by an elastic force, due to chain collapse, resulting in viscoelastic phase separation. Owing to these viscoelastic effects, the polymer-rich phase decreased its volume, which leads to the formation of macropores. A continuous change of the temperature during phase separation leads to the temporal change in the quench depth, which may cause secondary phase separation and the resulting multiscale structures.

3.5. Proposed Gelation Mechanism. Phase separation induced gelation is suggested as the mechanism for phase separation in aqueous solutions of cellulose ethers. Above the clouding temperatures, the solubility of polymers reduces due to the weakening of hydrogen bonds with increasing temperature. Spinodal decomposition gives rise to concentration fluctuations during phase separation; here the movement of polymer molecules is from low concentration to high concentration regions, causing the formation of an order structure with polymer-rich and polymer-poor phases. For simultaneous phase separation and gelation, "hydrophobic zones" connect polymer chains via hydrophobic aggregation in the polymer-rich phase, leading to the progressive formation of a continuous network. This leads to a pinned phase separation. However, if a thermal gap exists between phase separation and gelation, a water phase forms over the bicontinuous structure via secondary phase separation prior to gel formation. For both cases, turbid gels are always observed at high temperatures as they exhibit heterogeneous structures with sizes bigger than 1 μm.

4. CONCLUSION

Gelation coupled phase separation in aqueous solutions of MC and HPMC has been investigated by microscopy, rheology, and tubidimetry. In order to understand the complex thermal behavior, rheological measurements were used to test mechanical properties during the sol−gel transition, while independent optical microscopy and turbidimetry were used to probe the formation of phase-separated structures as a function of temperature. MC and HPMC solutions exhibit contrasting structural and rheological properties due to the differences in the interplay between phase separation and gelation.

In a 1.5 wt % A4M solution (MC), the growth of the modulus correlates well with the development of structure as phase separation and gelation proceed almost simultaneously. A bicontinuous structure formed via spinodal decomposition during phase separation with a domain length of ∼5 μm. Because of the pinning phenomenon, the structure did not growth with a further increase in temperature; i.e., phase separation was trapped by gelation at an initial stage. Although a thermal hysteresis existed between the heating and cooling processes, both gelation and phase separation were completely thermoreversible. G' returned to the original value after a complete thermal cycle, resulting in a dissolution of the bicontinuous structure.

In a 2 wt % E4M solution (HPMC), a significant drop in G' was observed at the clouding temperature; this result indicated that gelation took place after phase separation. A bicontinuous structure developed in the thermal gap between phase separation and gelation prior to an increase in G'. At a higher temperature, macropores formed over the bicontinuous structure via "viscoelastic phase separation" linked to secondary phase separation. The final turbid gel exhibited a complex ordered structure that consisted of a polymer-rich phase, a polymer-poor phase, and an additional water phase (or an exceedingly polymer-poor phase). In the subsequent cooling process, the macropores disappeared, followed by the dissolution of the bicontinuous structure at low temperatures. As for the MC system, this was also a reversible process.

■ AUTHOR INFORMATION

Corresponding Author

*E-mail: p.fairclough@sheffield.ac.uk (J.P.A.F.); yuhao07@gmail.com (H.Y.).

Present Address

⊥FujiFilm Imaging Colorants, Hexagon Tower, Blackley, Manchester M9 8ZS, UK.

Notes

The authors declare the following competing financial interest(s): HY was funded by The Dow Chemical Company.

■ ACKNOWLEDGMENTS

We acknowledge the financial support of the Dow Wolff Cellulosics business of The Dow Chemical Company for PhD funding (H.Y.) and the supply of materials. Additionally, we acknowledge the EPSRC and the Analytical Section of the Royal Society of Chemistry for PhD (O.K.). Finally, we also

express our gratitude and thanks to Professor Tanaka for useful discussions.

REFERENCES

(1) Nystroem, B.; Kjoniksen, A.-L.; Lindman, B. Effects of Temperature, Surfactant, and Salt on the Rheological Behavior in Semidilute Aqueous Systems of a Nonionic Cellulose Ether. *Langmuir* **1996**, *12*, 3233−3240.
(2) Karlberg, M.; Thuresson, K.; Piculell, L.; Lindman, B. Mixed solutions of hydrophobically modified graft and block copolymers. *Colloids Surf., A* **2004**, *236*, 159−164.
(3) Sanz, T.; Salvador, A.; Fiszman, S. M. Effect of concentration and temperature on properties of methylcellulose-added batters: Application to battered, fried seafood. *Food Hydrocolloids* **2003**, *18*, 127−131.
(4) Sanz, T.; Salvador, A.; Velez, G.; Munoz, J.; Fiszman, S. M. Influence of ingredients on the thermo-rheological behavior of batters containing methylcellulose. *Food Hydrocolloids* **2005**, *19*, 869−877.
(5) Barcenas, M. E.; Rosell, C. M. Effect of HPMC addition on the microstructure, quality, and aging of wheat bread. *Food Hydrocolloids* **2005**, *19*, 1037−1043.
(6) Miranda, A.; Millan, M.; Caraballo, I. Study of the critical points of HPMC hydrophilic matrices for controlled drug delivery. *Int. J. Pharm.* **2006**, *311*, 75−81.
(7) Sasa, B.; Odon, P.; Stane, S.; Julijana, K. Analysis of surface properties of cellulose ethers and drug release from their matrix tablets. *Eur. J. Pharm. Sci.* **2006**, *27*, 375−383.
(8) Chen, C.-H.; Tsai, C.-C.; Chen, W.; Mi, F.-L.; Liang, H.-F.; Chen, S.-C.; Sung, H.-W. Novel Living Cell Sheet Harvest System Composed of Thermoreversible Methylcellulose Hydrogels. *Biomacromolecules* **2006**, *7*, 736−743.
(9) Touitou, E.; Donbrow, M. Influence of additives on hydroxyethyl methyl cellulose properties: relation between gelation temperature change, compressed matrix integrity and drug release profile. *Int. J. Pharm.* **1982**, *11*, 131−48.
(10) Yang, L.; Kuang, J.; Wang, J.; Li, Z.; Zhang, L.-M. Loading and in vitro controlled release of indomethacin using amphiphilic cholesteryl-bearing carboxymethylcellulose derivatives. *Macromol. Biosci.* **2008**, *8*, 279−286.
(11) McCrystal, C. B.; Ford, J. L.; Rajabi-Siahboomi, A. R. Water Distribution Studies within Cellulose Ethers Using Differential Scanning Calorimetry. 2. Effect of Polymer Substitution Type and Drug Addition. *J. Pharm. Sci.* **1999**, *88*, 797−801.
(12) McCrystal, C. B.; Ford, J. L.; Rajabi-Siahboomi, A. R. Water Distribution Studies within Cellulose Ethers Using Differential Scanning Calorimetry. 1. Effect of Polymer Molecular Weight and Drug Addition. *J. Pharm. Sci.* **1999**, *88*, 792−796.
(13) Pourchez, J.; Peschard, A.; Grosseau, P.; Guyonnet, R.; Guilhot, B.; Vallee, F. HPMC and HEMC influence on cement hydration. *Cem. Concr. Res.* **2006**, *36*, 288−294.
(14) Weyer, H. J.; Mueller, I.; Schmitt, B.; Bosbach, D.; Putnis, A. Time-resolved monitoring of cement hydration: Influence of cellulose ethers on hydration kinetics. *Nucl. Instrum. Methods Phys. Res., Sect. B* **2005**, *238*, 102−106.
(15) Sarkar, N. Thermal gelation properties of methyl and hydroxypropyl methylcellulose. *J. Appl. Polym. Sci.* **1979**, *24*, 1073−87.
(16) Hirrien, M.; Chevillard, C.; Desbrieres, J.; Axelos, M. A. V.; Rinaudo, M. Thermal gelation of methyl celluloses: new evidence for understanding the gelation mechanism. *Polymer* **1998**, *39*, 6251−6259.
(17) Vigouret, M.; Rinaudo, M.; Desbrieres, J. Thermogelation of methyl cellulose in aqueous solutions. *J. Chim. Phys. Phys.-Chim. Biol.* **1996**, *93*, 858−869.
(18) Li, L. Thermal gelation of methylcellulose in water: Scaling and thermoreversibility. *Macromolecules* **2002**, *35*, 5990−5998.
(19) Lam, Y. C.; Joshi, S. C.; Tan, B. K. Thermodynamic characteristics of gelation for methyl-cellulose hydrogels. *J. Therm. Anal. Calorim.* **2007**, *87*, 475−482.
(20) Haque, A.; Morris, E. R. Thermogelation of methylcellulose. Part I: Molecular structures and processes. *Carbohydr. Polym.* **1993**, *22*, 161−73.
(21) Haque, A.; Richardson, R. K.; Morris, E. R.; Gidley, M. J.; Casell, D. C. Thermogelation of methylcellulose. Part II: Effect of hydroxypropyl substituents. *Carbohydr. Polym.* **1993**, *22*, 175−86.
(22) Sarkar, N. Kinetics of thermal gelation of methyl cellulose and hydroxypropyl methyl cellulose in aqueous solutions. *Carbohydr. Polym.* **1995**, *26*, 195−203.
(23) Kobayashi, K.; Huang, C.-i.; Lodge, T. P. Thermo-reversible gelation of aqueous methyl cellulose solutions. *Macromolecules* **1999**, *32*, 7070−7077.
(24) Mark, H. F. Cellulose ethers. *Encycl. Polym. Sci. Technol.* **2004**, 507−531.
(25) Takeshita, H.; Saito, K.; Miya, M.; Takenaka, K.; Shiomi, T. Laser Speckle Analysis on Correlation between Gelation and Phase Separation in Aqueous Methyl Cellulose Solutions. *J. Polym. Sci., Part B: Polym. Phys.* **2010**, *48*, 168−174.
(26) Villetti, M. A.; Soldi, V.; Rochas, C.; Borsali, R. Phase-Separation Kinetics and Mechanism in a Methylcellulose/Salt Aqueous Solution Studied by Time-Resolved Small-Angle Light Scattering (SALS). *Macromol. Chem. Phys.* **2011**, *212*, 1063−1071.
(27) Kita, R.; Kaku, T.; Kubota, K.; Dobashi, T. Pinning of phase separation of aqueous solution of hydroxypropyl methyl cellulose by gelation. *Phys. Lett. A* **1999**, *259*, 302−307.
(28) Kita, R.; Kaku, T.; Ohashi, H.; Kurosu, T.; Iida, M.; Yagihara, S.; Dobashi, T. Thermally induced coupling of phase separation and gelation in an aqueous solution of hydroxypropylmethylcellulose (HPMC). *Phys. A (Amsterdam, Neth.)* **2003**, *319*, 56−64.
(29) Bodvik, R.; Dedinaite, A.; Karlson, L.; Bergstrom, M.; Baverback, P.; Pedersen, J. S.; Edwards, K.; Karlsson, G.; Varga, I.; Claesson, P. M. Aggregation and network formation of aqueous methylcellulose and hydroxypropylmethylcellulose solutions. *Colloids Surf., A* **2010**, *354*, 162−171.
(30) Hussain, S.; Keary, C.; Craig, D. Q. M. A thermorheological investigation into the gelation and phase separation of hydroxypropyl methyl cellulose aqueous systems. *Polymer* **2002**, *43*, 5623−5628.
(31) Silva, S. M. C.; Pinto, F. V.; Antunes, F. E.; Miguel, M. G.; Sousa, J. J. S.; Pais, A. Aggregation and gelation in hydroxypropylmethyl cellulose aqueous solutions. *J. Colloid Interface Sci.* **2008**, *327*, 333−340.
(32) Heymann, E. Sol-gel transformations. I. The inverse sol-gel transformation of methylcellulose in water. *Trans. Faraday Soc.* **1935**, *31*, 846−64.
(33) Flory, P. J. Introductory lecture. *Faraday Discuss. Chem. Soc.* **1974**, *57*, 7−18.
(34) Te Nijenhuis, K. *Adv. Polym. Sci.* **1997**, *130*, 4.
(35) Guenet, J. M. *Thermoreversible Gelation of Polymers and Biopolymers*; Academic Press: London, 1993.
(36) Clark, A. H.; Ross-Murphy, S. B. Structural and Mechanical properties of biopolymer gels. *Adv. Polym. Sci.* **1987**, *83*, 60−181.
(37) Rossmurphy, S. B. Structure-property relationships in food biopolymer gels and solutions. *J. Rheol.* **1995**, *39*, 1451−1463.
(38) Keller, A. Aspects of polymer gels. *Faraday Discuss.* **1995**, *101*, 1−49.
(39) Spevacek, J.; Schneider, B. Aggregation of stereoregular poly(methyl methacrylates). *Adv. Colloid Interface Sci.* **1987**, *27*, 81−150.
(40) Tohyama, K.; Miller, W. G. Network structure in gels of rod-like polypeptides. *Nature* **1981**, *289*, 813−814.
(41) Li, L.; Wang, Q.; Xu, Y. Thermoreversible association and gelation of methyl cellulose in aqueous solutions. *Nihon Reoroji Gakkaishi* **2003**, *31*, 287−296.
(42) Xu, Y.; Li, L. Thermoreversible and salt-sensitive turbidity of methylcellulose in aqueous solution. *Polymer* **2005**, *46*, 7410−7417.
(43) Seeton, C. J. Viscosity-temperature correlation for liquids. *Tribol. Lett.* **2006**, *22*, 67−78.
(44) Ferry, J. D. *Viscoelastic Properties of Polymers*, 3rd ed.; Wiley: New York, 1980; p 641.
(45) Jones, R. A. L. *Soft Condensed Matter*; Oxford University Press: Oxford, 2002; p 195.

(46) Tanaka, H. Viscoelastic phase separation. *J. Phys.: Condens. Matter* **2000**, *12*, 207−264.
(47) Tanaka, H. Formation of Network and Cellular Structures by Viscoelastic Phase Separation. *Adv. Mater.* **2009**, *21*, 1872−1880.